We are IntechOpen,
the world's leading publisher of
Open Access books
Built by scientists, for scientists

4,800
Open access books available

122,000
International authors and editors

135M
Downloads

Our authors are among the

154
Countries delivered to

TOP 1%
most cited scientists

12.2%
Contributors from top 500 universities

CLARIVATE ANALYTICS
BOOK CITATION INDEX
INDEXED

WEB OF SCIENCE™

Selection of our books indexed in the Book Citation Index
in Web of Science™ Core Collection (BKCI)

Interested in publishing with us?
Contact book.department@intechopen.com

Numbers displayed above are based on latest data collected.
For more information visit www.intechopen.com

Quantum Dot Composite Radiation Detectors

Mario Urdaneta[1], Pavel Stepanov[1], Irving Weinberg[1],
Irina Pala[2] and Stephanie Brock[2]
[1]Weinberg Medical Physics LLC
[2]Wayne State University
USA

1. Introduction

Inspired by experimental high-energy physics experiments, the first radiation detectors in positron emission tomography (PET), computer tomography (CT), and gamma-cameras were built of scintillators combined with vacuum phototubes (e.g., photomultipliers, photodiodes). Fifty years later, the scintillators/photomultiplier approach has matured, but still has intrinsic limitations. Vacuum phototubes are relatively bulky. Photomultipliers require high voltage (e.g., 0.5-2.5 kV). Vacuum phototubes are delicate because of fragile glass or quartz windows (a requisite for light to enter the vacuum tube) and fine-gap electrode structures (e.g., dynodes, grid and anode) suspended within the vacuum. Photocathodes can be irreversibly damaged if the photomultiplier is powered under normal lighting conditions. Most types of vacuum photodetectors are sensitive to external magnetic fields and therefore require magnetic shielding for certain environments (e.g., inside Magnetic Resonance Imaging systems). Vacuum phototube aging is often another challenge, because over time, vacuum inside photomultipliers tube degrades, resulting in performance degradation (e.g., increasing noise).

Today, the scintillator/vacuum phototube combination is being replaced by the scintillator/solid state photomultiplier combination (e.g., Multi-Pixel Photon Counter by Hamamatsu or Silicon Photomultipliers by SensL). Solid state photomultipliers address some of the limitations of vacuum phototubes. For example, solid state photodetectors have small size, do not require high voltage, are more robust mechanically, and are compatible with strong magnetic fields. However, they bring new challenges: higher noise and very high sensitivity to temperature and supply voltage variations. Even more importantly, solid state photodetectors do not address main challenges in radiation detection (e.g., the need for better sensitivity and better energy and spatial resolution), because the approach still depends on the same scintillators and thus involves a multi-step process for converting radiation to signal: using scintillators to convert radiation to visible light, then transporting the light into the photodetector, which finally converts light into electrical signals. A better alternative is the use of direct-conversion radiation detectors.

Direct conversion detectors are detectors in which radiation is converted directly into electrical signals. Most commonly, such detectors are made of semiconductors. There is usually an electrical bias applied to the semiconductor. Photons that interact with the semiconductor generate electron-hole pairs. Moving electrons and holes generate electrical signal in the form of increased semiconductor current. The simplest example of such a radiation detector is a silicon diode. While direct radiation detectors offer potential benefits of improved energy and spatial resolution, they have reduced detection efficiency (or "stopping power") as compared to many scintillators, especially for high energy radiation (e.g., radiation with energy above 100 keV).

In order to minimize patient radiation dose in medical imaging, it is helpful to increase stopping power, since stopping power is inversely related to the dose required for obtaining high quality patient images. High stopping power also enables the detector length to be reduced, improving spatial resolution (due to lower depth-of-interaction error) (Nassalski et al., 2007). Employing composite solid-state detectors with high stopping power as components would significantly reduce size, weight, and power requirements for imaging systems, and decrease the dose required to perform high-quality radiological examinations. As an example, we previously published a design for a PET-enabled glove, which would be difficult to implement using the current generation of vacuum phototubes (Wong et al., 2006). Detection efficiency is proportional to the fifth power of the effective atomic number (for photoelectric absorption). Therefore semiconductor type materials with high effective atomic number have the potential for developing efficient direct-converting radiation detectors.

Using the effective atomic numbers for various materials, Table 1 lists an estimate of the relative dose that would be required to collect satisfactory images using diagnostic radiologic equipment (Jackson and Hawkes, 1981).

In order to utilize the electrical signal produced by radiation (e.g., electron-hole pairs), one needs to be able to transport charge carriers through the semiconductor into electrodes at the edges of the detector. Therefore, a semiconductor with high mobility and lifetime for charge carriers is needed for radiation detection applications. For common semiconducting materials, high atomic number and good charge transport properties are not generally found together. For example, silicon has excellent charge transport properties but a low atomic number, $Z = 14$, which makes the silicon efficient only for low energy radiation detection (e.g., radiation with energy ≤ 10keV). The current generation of solid-state direct-conversion radiation detectors utilizes cadmium zinc telluride ("CZT", effective atomic number $Z = 48$), or cadmium telluride (effective atomic number $Z = 50$) (Liu et al., 2000). Unfortunately, elements with higher stopping powers (e.g., Pb, $Z = 82$) do not form compounds with the transport properties (e.g., mobility-lifetime product) that would be favorable for direct-conversion detectors (Perkins et al., 2003).

One material that would be attractive as a direct conversion material is lead sulfide (PbS, with an effective atomic number of $Z = 77$) because it is a semiconductor and because its relatively populated electron cloud increases the likelihood of photon-electron interaction. The bulk form of PbS has a small band gap (0.2 and 0.41 eV for 4 K and 293 K respectively) (Hoffmann and Pentel, 2000), and this results in a large dark current (due to thermally generated charge carriers). It is possible to engineer the material to have a larger band gap by making quantum dots (QD) of the material (Steigerwald and Brus, 1990). Engineering the

band gap enables PbS to be used as a practical material in radiation detection when the noise levels is of concern (e.g., spectroscopy, low photon count conditions). The effective band gap of a quantum dot (Fig. 1) depends on the quantum dot size, and the solution to the Schrödinger equation for the quantum dot excited state can be approximated to relate the quantum dot size and its band gap (Nedelikovic et al., 1993). We have examined the use of QDs in host matrices that combine the transport properties of the host material with the band-gap and stopping power properties of PbS QDs.

Material	Effective Atomic Number	Relative Dose Requirement
Lanthanum bromide	47	100%
Cadmium zinc telluride	48	95%
Sodium iodide	50	86%
Cadmium telluride	50	86%
Cesium iodide	54	70%
Lutetium yttrium orthosilicate	66	43%
Lead sulfide	77	29%

Table 1. Expected Dose Reduction. Estimated patient dose required for collection of equal signal-to-noise ratios, in molecular imaging systems utilizing equally-long samples of radiodetector materials, in comparison with lanthanum bromide (one of the best scintillator options available). The effective atomic number for composite materials was calculated using published methods (Taylor et al., 2009). The relative dose requirement is computed by taking the fifth power of the ratios of effective atomic numbers (to get the relative efficiency at detecting gamma radiation via photoelectric absorption) and then taking the square root (to get the relative noise, which goes as the root of the number of photons collected), and then inverting to get the relative dose requirement. For PET, the relative dose requirement would be even more pronounced than in Table 1, since the efficiency is squared in a coincident measurement. The numbers shown illustrate the motivation for increasing the atomic number.
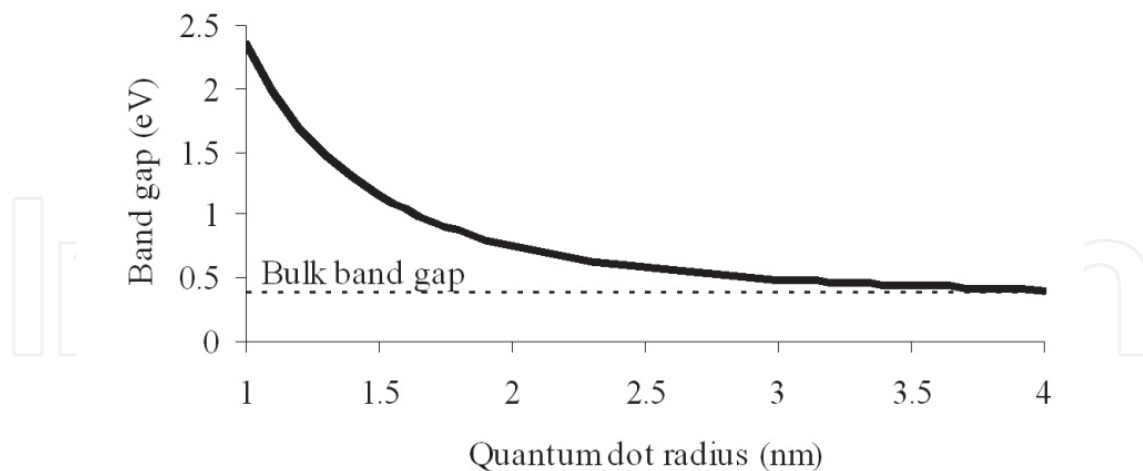
Fig. 1. Relationship between the size of lead sulfide (PbS) quantum dots and their electronic band gap.

2. Approach and methodology

Previous approaches to quantum dot radiation detectors have used indirect conversion of the radiation. In these QD-enabled detectors, the quantum dots act as scintillators to generate light pulses upon impingent radiation. The pulses are then recorded by photomultipliers (Campbell and Crone, 2005). Instead of the indirect approach, we chose to pursue a direct-conversion route, which holds the promise of better energy resolution. Our initial effort was inspired by photovoltaic research suggesting the use of organic semiconductors as host materials to quantum dots that sensitized the material to wavelengths of interest (Schwenn et al., 2005). Although these prior efforts were able to produce quantum dot/organic semiconductor films 1 μm thick, such thicknesses would only be appropriate for capturing low-penetration radiation (e.g., visible light or alpha particles). Thicker films would be necessary in order to stop incoming radiation of high enough energies to be of interest to the medical or defense fields. Additionally, organic semiconductors have reduced charge transport performance (as compared to inorganic semiconductors), and deteriorate as a result of both oxygen and the impinging radiation they are supposed to detect. We therefore pursued a novel approach involving porous and micromachined silicon as a matrix for a quantum dot composite material. The approach of using silicon as a matrix is easier to implement than using organic semiconductors, because of a reduced requirement for an oxygen-free environment during fabrication of the detector. The combination of quantum dots and porous silicon resulted in the prototype detector schematically shown in Figure 2. In some respects, the detector is very similar in geometry and operation to other direct conversion radiation detectors: it is comprised of a planar semiconductor material with electrodes on the top and bottom faces; a reverse bias on the electrodes depletes the semiconductor material and electrons and holes are collected at the electrodes. The main difference is that the detecting portion of the device is nano-engineered to maximize the production and collection of electrons and holes in the presence of high energy radiation.
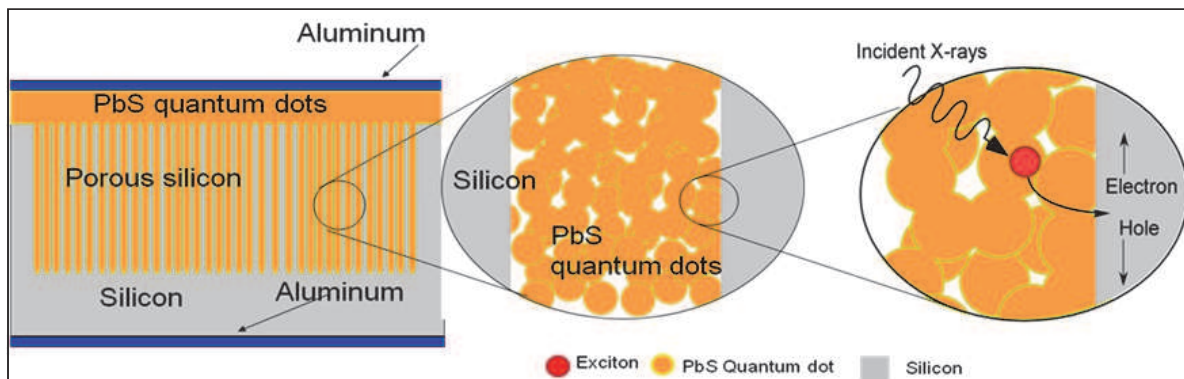
Fig. 2. Quantum dot/silicon device. Device design on left, illustrates that when incident photons interact with the lead sulfide quantum dots, excitons are produced, which in turn are separated into an electron and hole at heterojunctions (i.e., junctions between dissimilar materials). An externally applied electric field draws the electrons and holes towards aluminum electrodes, which causes an increase in the current through the device.

The generation and disassociation of excitons is a critical step (Sambur et al., 2010) in the detection of radiation in quantum-dot based devices. Excitons are disassociated into electrons and holes when they meet a heterojunction (a junction of two materials with different electronic structures) because of the sudden electrostatic field at the interface of the two materials. The resulting electrons and holes can be manipulated using electric fields as in traditional semiconductor detectors. It is of critical interest to maximize the probability of exciton to electron-hole-pair conversions in order to have good conversion efficiencies. Once electrons and holes are generated, these charge carriers have to travel to the readout electrodes. Lead sulfide, in both bulk and quantum dot forms, has sub-optimal charge mobilities and lifetimes. Making matters worse, our interest in radiation detection means that we desire detectors with large charge carrier travel paths (we need thick detectors so that they can stop radiation of very high energy, e.g., 4.4 MeV). Thus, charge transport is a critical factor in the realization of detectors for high-energy radiation. We address both challenges, charge transport and exciton disassociation, by using porous silicon as a host material for the PbS quantum dots.

Porous silicon is a nanostructured material that consists of silicon (in crystalline form, typically) which has been electrochemically treated in a hydrofluoric acid-rich solution to have pores of size ranging between one and hundreds of nanometers (Foll et al., 2002, Lehmann et al., 2000). We processed a silicon wafer in order to obtain porous silicon with straight holes, of diameter 100 nm, normal to the surface of the silicon wafer and along the crystal direction <100>. Figure 3 shows an overhead view of one of our silicon wafers after such processing. The depth of the pores is a function of processing conditions and the properties of the silicon. Pores up to 1 mm deep have been reported (Holke and Henderson, 1999). In the experimental results presented we used a porous silicon layer 20 μm thick, and used additional micromachining techniques to achieve effective layers 700 μm thick.

The quantum dots that were employed in the experiments presented were manufactured in-house using solution-phase methods under inert conditions (Hines and Scholes, 2003). The quantum dots were capped with oleic acid and dispersed in hexane. Each batch of quantum dots was characterized using photoluminesence and photoabsorbance data. Typically, absorbance and emission peaks occur around 800 nm, corresponding to a band gap of about

1.3 eV (Figures 4A and B). This band gap is consistent with a quantum dot size of 2 – 3 nm in diameter, which is consistent with both transmission electron microscopy (TEM) images of the quantum dots (Figure 4C) and literature models. Powder X-ray diffraction (PXRD) data revealed that the quantum dots adopted the cubic PbS crystal structure (Figure 4D).
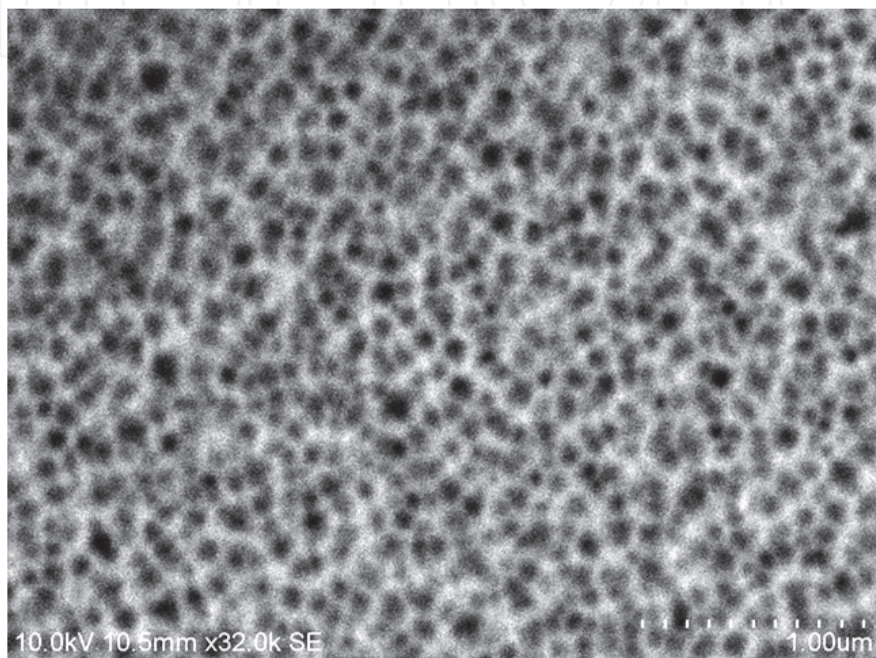

Fig. 3. Overhead view of the porous silicon used in the radiation detectors described. The holes are normal to the surface of the wafer, along the <100> crystal direction, which is preferentially weak to the attack of the anodization process.

The quantum dots were loaded into the porous silicon by capillary action. The surface of freshly treated porous silicon is hydrophobic, and is wetted by the organic solvent solution in which the quantum dots are dispersed. We verified that the quantum dots entered the entire depth of the pores by cleaving a PbS loaded section of porous silicon and performing electron energy dispersive spectroscopy on the cross-section. An image of such cross-section is shown in Figure 5. Distinct regions of elemental silicon, elemental lead, and a region that includes both (the quantum dot-laden portion of the porous silicon) are clearly visible, with lead reaching the full depth of the region of porous silicon. Once loaded, aluminum was evaporated on top of the quantum dot layer, which makes up one of the two electrical contacts in the detector (the other contact consists of aluminum evaporated on the opposite side of the silicon wafer).
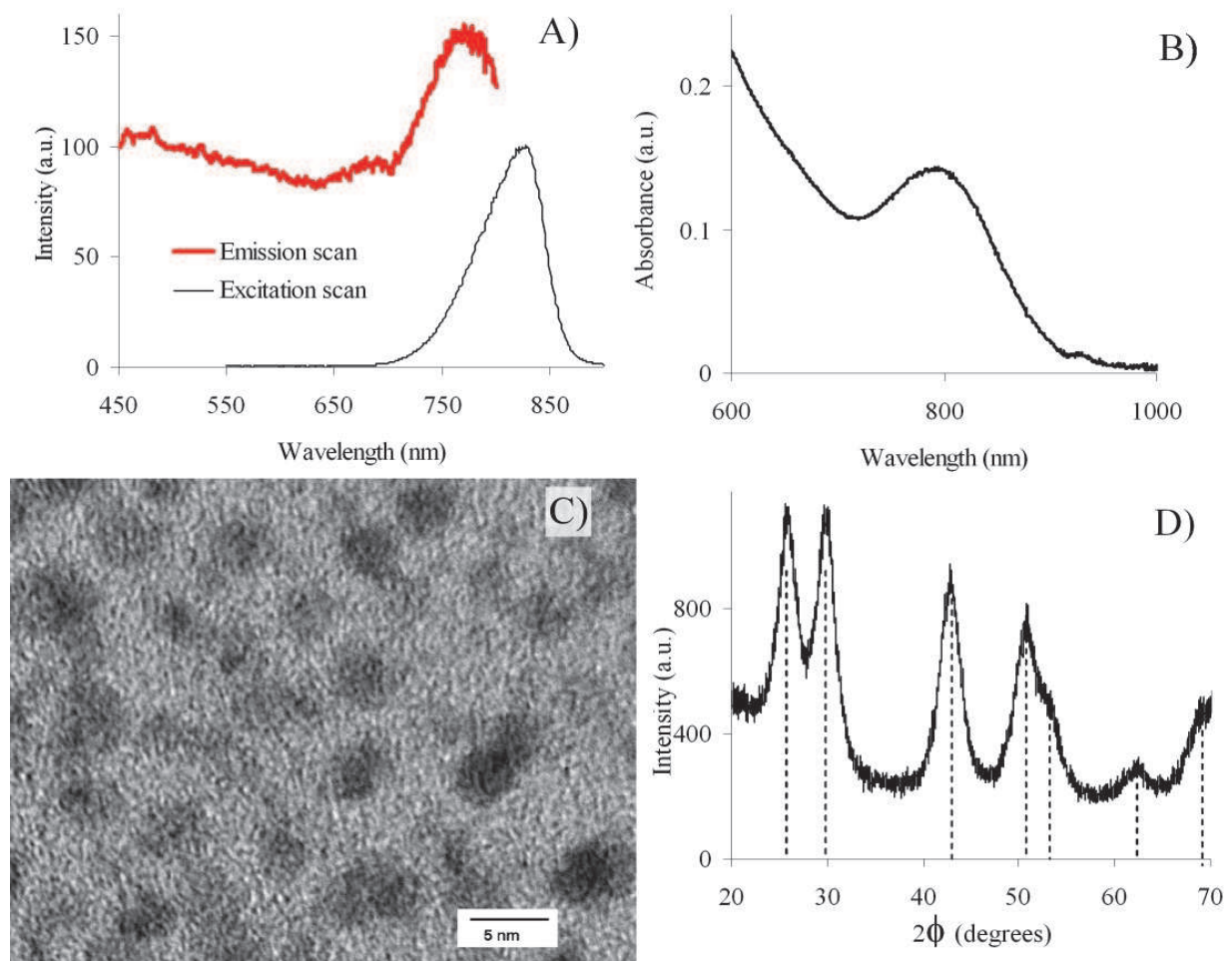
Fig. 4. The characterization of the quantum dots used in the radiation detectors include (A) photoluminesence, which in this case shows a peak at 827 nm, (B) absorbance, which in this case shows an absorption peak at 794 nm, (C)TEM images, showing quantum dots of various sizes, and (D) PXRD data of the PbS nanoparticles, showing the cubic lead sulfide structure.
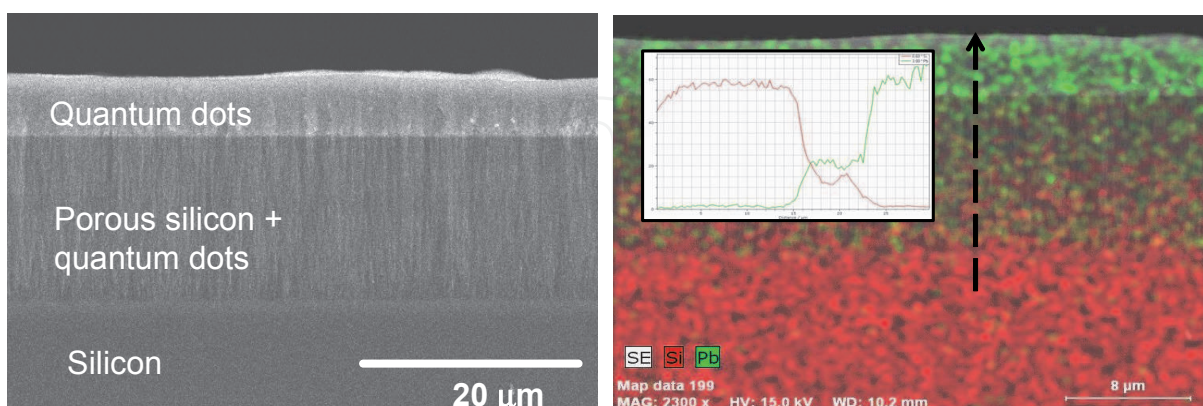

Fig. 5. (Left) Cross-sectional backscattered electron micrograph of the active region of the detector. (Right) Energy dispersive spectroscopy map of the same region showing the distribution of lead (green) and silicon (red). Regions of pure PbS, non-porous silicon, and the composite PbS/porous silicon (mixed green-red) are evident. The insert shows the proportions of silcon and lead along the length of the dashed arrow.

The detector was reverse biased at 1.6V and connected to an operational amplifier in the classical configuration illustrated in Figure 6.
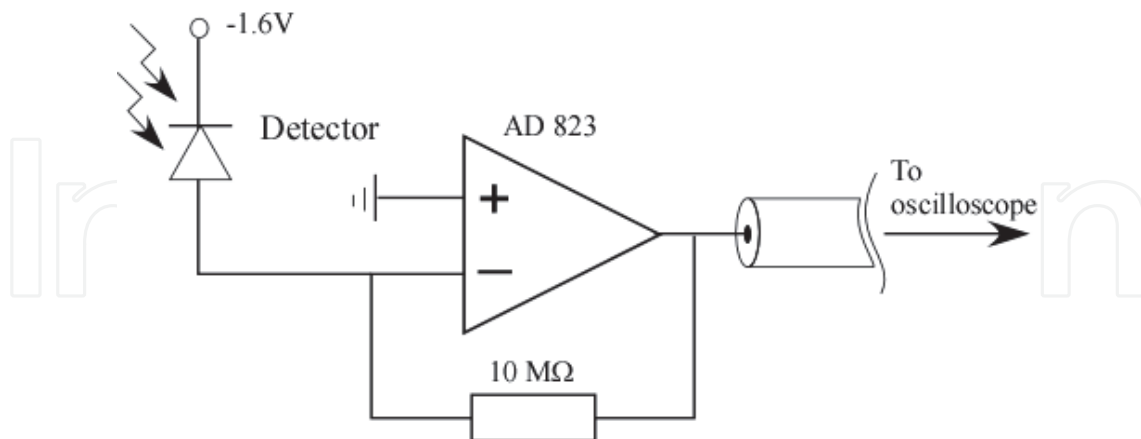
Fig. 6. Connection diagram of the detector during testing and operation.

3. Experimental results

In order to test the detector under relevant clinical conditions, we exposed it to x-rays produced by a CT scanner at various energy levels. A typical detector response is shown in Figure 7. One can see the effect of the attenuation of the x-rays reaching the detector after they have passed through the various materials that make up the detector housing (Figure 7 insert shows the CT-acquired image of the detector housing, with the detector itself pointed by the arrow). The detector also showed good radiation hardness, by having a response that remained the same even after exposure to over 11 Gy of x-ray radiation, equivalent to 3000 mammograms.
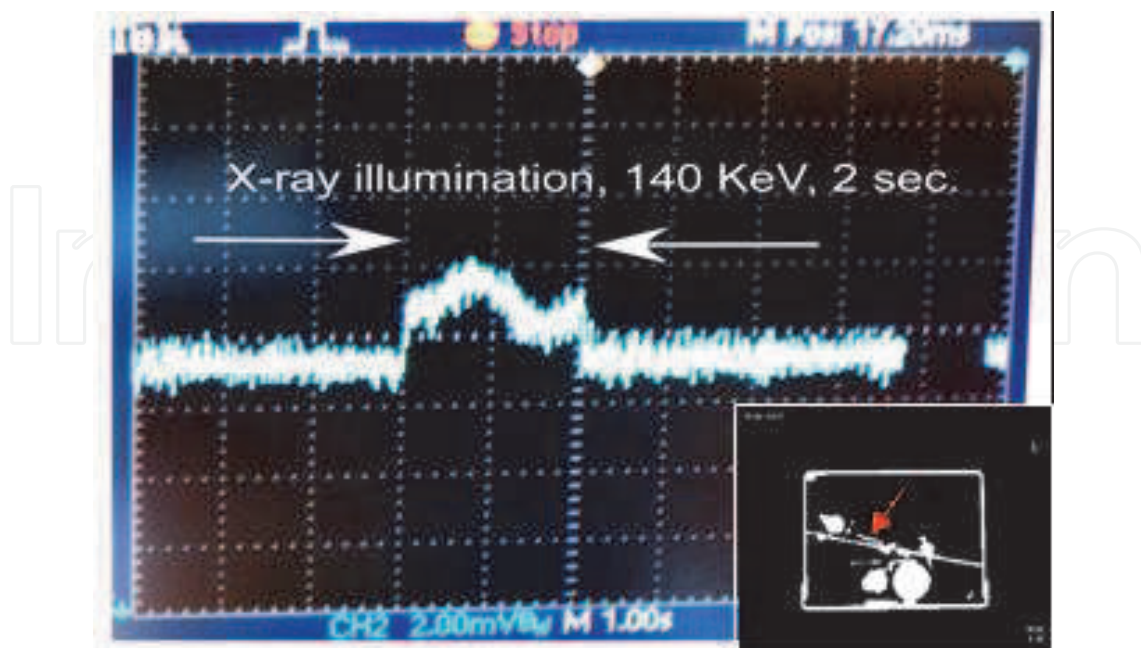
Fig. 7. Radiation Response Characterization. X-ray response of composite material, unchanged after exposure to equivalent of 3000 x-ray mammograms.

The detector response to the intensity of the radiation beam is linear, as evidenced in Fig. 8. Such linearity is required for clinical radiography.
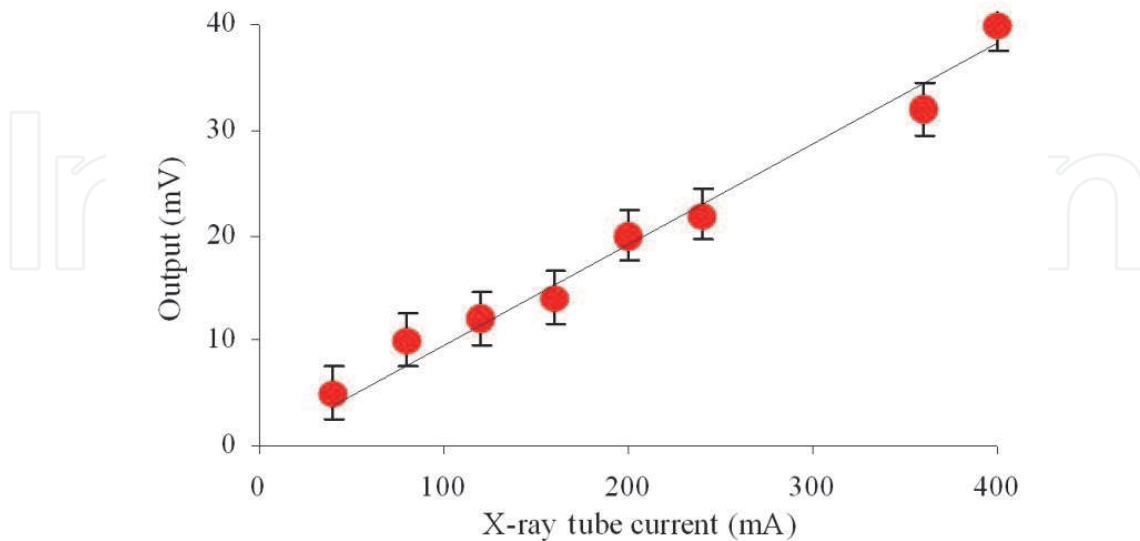

Fig. 8. Detector output response to x-rays of 120 keV at various intensities (tube currents).

The detection of radiation is intimately related to the ability of the detector material to stop the radiation. We expected our detector to attenuate x-ray radiation better than common radiation direct-conversion materials (e.g., Si, CdTe, CZT), and we verified this by blocking the radiation window of a bismuth germinate orthosilicate (BGO) scintillator coupled to a photomultiplier with a PbS/pSi detector (no housing). We exposed the detector to x-rays at various energies while monitoring the photomultiplier output, in order to obtain the relative attenuation (with and without the sample).
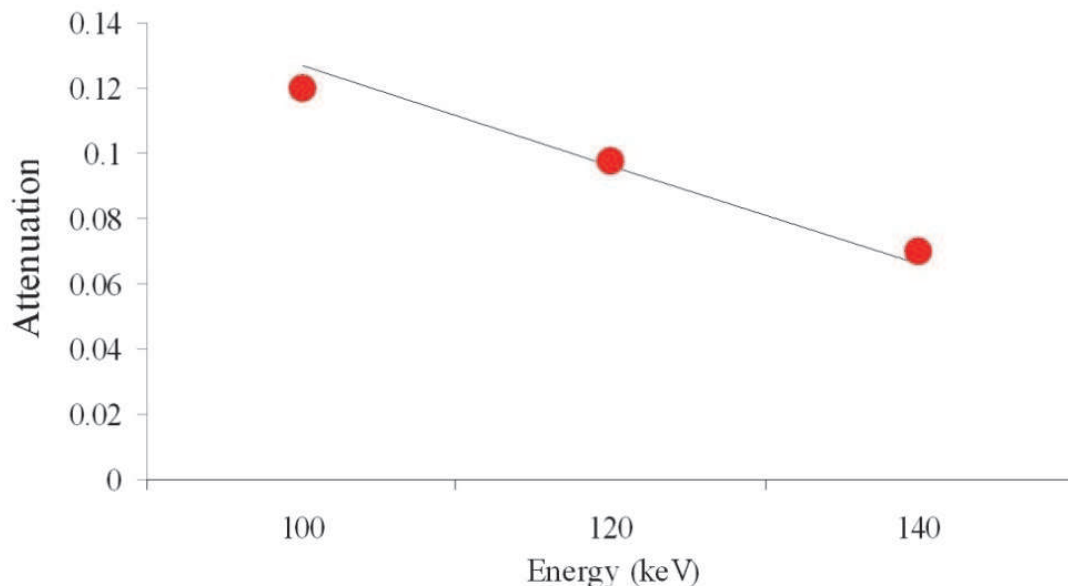

Fig. 9. X-ray Attenuation. We compare experimental attenuation values (circles) of layers of composite material to expected NIST-derived attenuation coefficients (black line). The linear attenuation coefficient was higher than CdTe, CZT.

Figure 10 shows measurements of mobility-lifetime product and resistivity from decay lifetime measurements. Mobility-lifetime (ML) was calculated to be 10^{-4} cm^2/V, using the relation

$$ML = (d^2/V)*(\tau_{lifetime}/\tau_{transition});$$

where $\tau_{lifetime}$ is lifetime for charge carries and $\tau_{transition}$ is time needed for charge carries to go across the device thickness d under applied bias voltage V. Mobility-lifetime measurements were obtained using published methods (Schwenn et al., 2005), in response to a fast (250 ns) laser pulse of infrared radiation (900 nm), and to ambient light. Resistivity measurements, measured by recording the leakage current while the detector is in reverse bias in the dark, show that the average value is 3 x 10^{10} Ω-cm. These values are within acceptable ranges for radiation detection (Owens and Peacock, 2004).

The detector also shows response to visible radiation (in addition to infrared), as would be expected based on the band gap of the PbS quantum dots employed. We measured the detector response to white light (white-LED flash light) as a function of bias, and found a strong dependance on illumination, especially in the forward bias condition. An example of detector response to light, as a function of bias, is shown in Figure *11*.
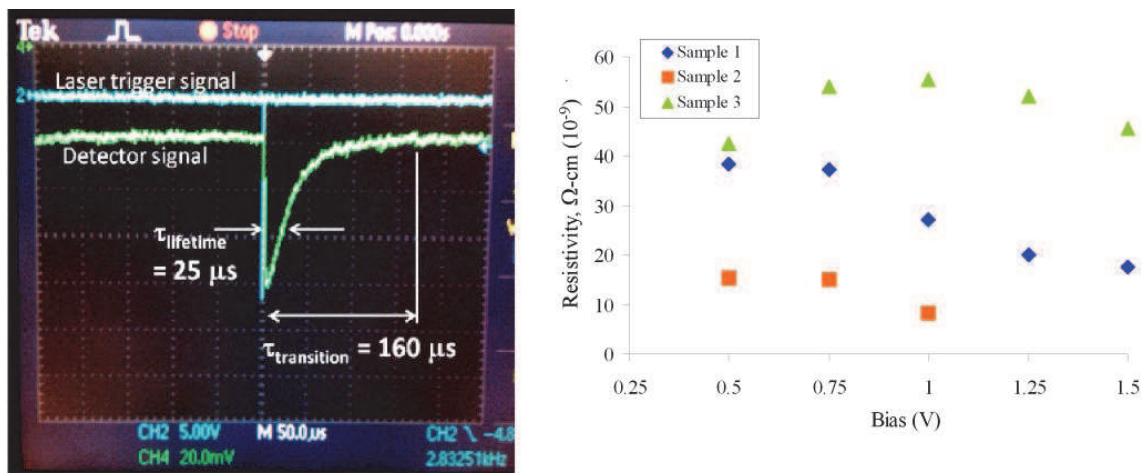

Fig. 10. (Left) Mobility-lifetime measurement using published methods (Schwenn et al., 2005), in response to a fast (250 ns) laser pulse of infrared radiation. (Right) Resistivity of the PbS/porous Si material as a function of reverse bias.
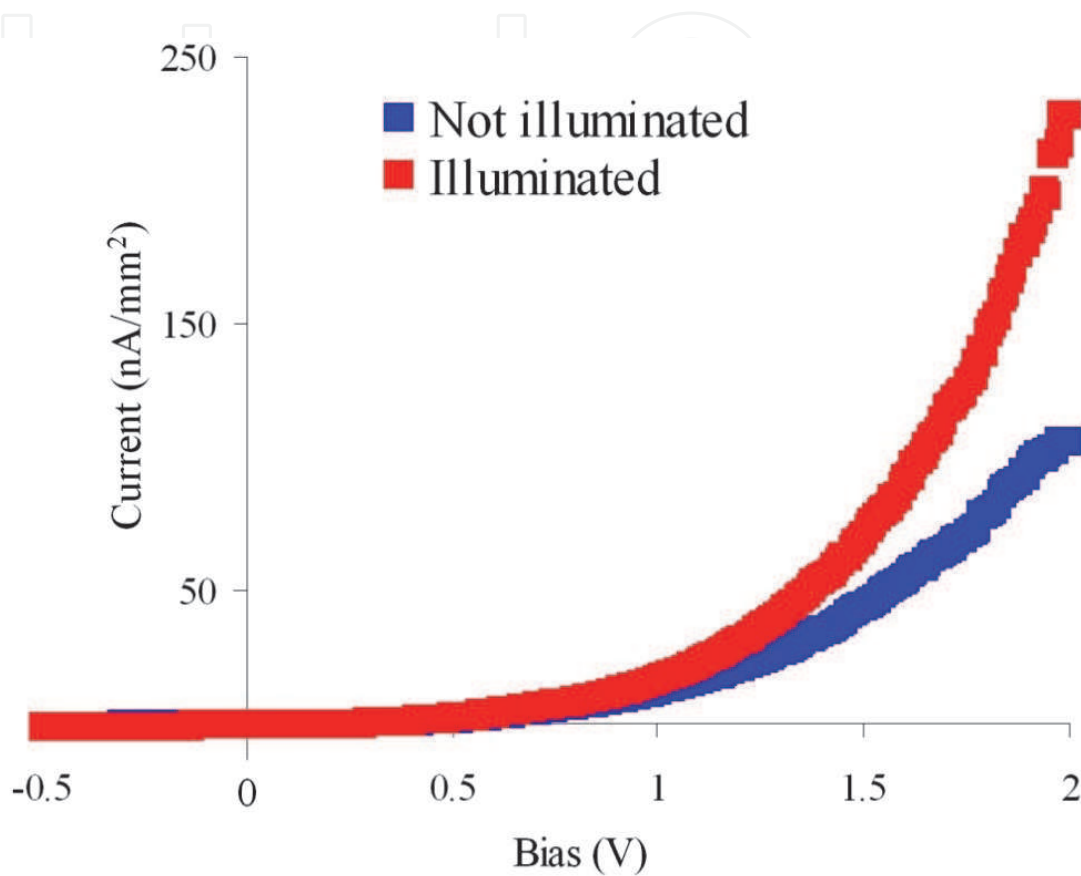
Fig. 11. Visible light sensitivity: The I-V curve shows response to visible light (white LED).

It is important to note that each experiment included control detectors consisting of silicon pieces treated the same way as the detectors but without being loaded with quantum dots. None of the control devices showed any response to any type of radiation.

4. Discussion

The detector presented is the result of the combination of two nano-engineered materials. This combination is notable as an important technical milestone: unlike classic rules concerning composite radiodetection materials (Owens and Peacock, 2004), it may now be possible to separate the problem of charge transport from that of charge conversion.

In this work, we presented the use of porous silicon as a host for quantum dots in a radiation detector. An attractive aspect of working with porous silicon is that the crystalline structure of the silicon remains intact, and thus the charge transport characteristics of the silicon remain relatively unaffected. In addition to improved charge transport, we expected that porous silicon would aid in increasing the conversion fraction of excitons to electron-hole pairs. This is because excitons travel a limited range (~20 nm) before they recombine and dissipate their energy, with lifetime of about one microsecond (Moreels et al., 2009). Thus, only the quantum dots whose distance from a heterojunction within an exciton's range will result in the appearance of electronic signals from the composite detector. Quantum dots deposited as a planar film, however thick the film is, will only yield signals coming from the quantum dots in the volume within exciton range of the silicon-QD interface (Winder and Sariciftci, 2004). In contrast, QDs deposited within a porous silicon matrix will be able to yield much larger signals (for a given device footprint) because the volume of QDs within exciton range of the QD-silicon interface is much greater. For the case of pores of about 100 nm in diameter, most of the QDs in the pore will be within exciton range of the heterojunction. Thus, the effective layer of quantum dots that are active participants in detection grows dramatically (i.e., from 20 nm to >20 μm).

This new nanotechnology-enabled paradigm promises to confer flexibility to future material designers, who will be able to increase effective atomic number and band-gap with less concern about impairing the material's ability to transport charge (e.g., mobility-lifetime product). The detector involves innovations at multiple scales of fabrication, from the nano-level (in the production of quantum dots), to the micro-level (in the fabrication of silicon micro-structures to accommodate the quantum dots and to amplify signals), to the macro-level (as imaging devices are designed to take advantage of favorable absorption properties). Under this new paradigm, it is easy to imagine the incorporation of quantum dots with different band-gap properties into a single silicon system, capable of detecting broad swaths of the electromagnetic spectrum. The concept of a single detector to sense multiple spectral domains (infrared, visible, x-ray) might be attractive to designers of night-vision goggles and viewfinders, who currently use separate cameras to image visible and infrared features for surveillance uses by soldiers and first-responders. The ability to place amplifiers and buffers on the same wafer as the sensor is very important to designers of focal-plane arrays, who are currently forced to hybridize detectors with bump-bonding methods that limit spatial resolution and are vulnerable to temperature changes (due to differing thermal-expansion characteristics of the bonded strata). The use of a silicon platform also satisfies designers who wish to put as much digital logic as possible in close proximity to the detectors, as has been done for silicon photomultipliers. An illustration of the flexibility of the platform is shown in Figure 12.

Currently, many PET, SPECT, CT scanners and digital mammography and radiography systems employ small scintillating crystals to detect radiation. Such crystals take weeks to grow, devour considerable energy, and may deplete supplies of rare elements. As an example, lutetium orthosilicate (widely used in the PET industry) melts at 2,150 °C, requiring iridium crucibles which must be recast frequently. The low-cost quantum dot methods we are investigating (which might utilize dip vats or spray processes to create and deposit the the QDs) could potentially replace the need to grow crystals.
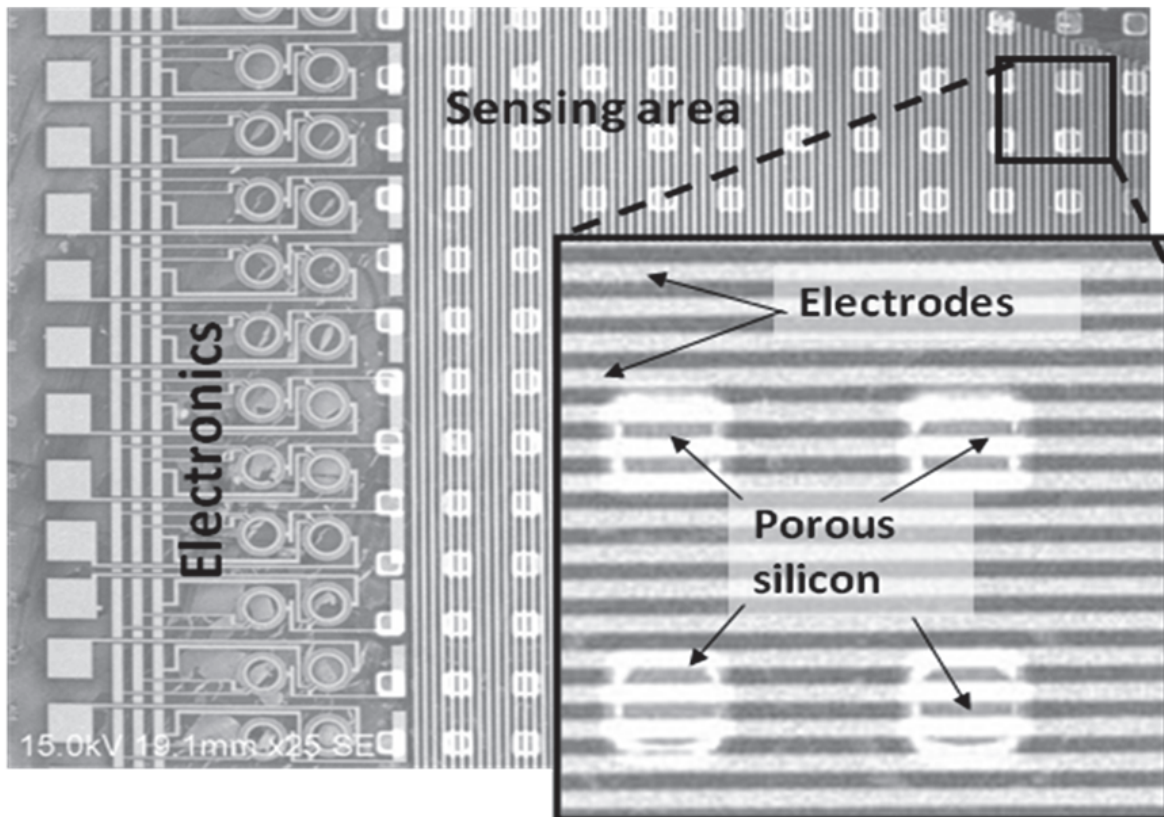
Fig. 12. Electronic test structures. By masking the material before creating the pores, we could include electronic features on the same wafer as the sensor.

5. Conclusions

This project represents an early application of nanotechnology to radiation detection. The innovation promises to reduce radiation dose and health care costs and improve radiological device performance. In addition to the diagnostic radiology market, the platform technology may be useful for homeland security and broad-spectrum surveillance for the consumer and defense markets, with potential cross-fertilization to the solar power industry.

6. Acknowledgment

7. References

Campbell, I. H. & Crone, B. K. 2005. Quantum-Dot/Organic Semiconductor Composites For Radiation Detection. *Adv. Mat.*, 18, 77-79.
Foll, H., Christophersen, M., Carstensen, J. & Hasse, G. 2002. Formation And Application Of Porous Silicon. *Mat. Sci. Engr. R*, 39, 93 - 141.

Hines, M. A. & Scholes, G. D. 2003. Colloidal PbS Nanocrystals With Size-Tunable Near-Infrared Emission: Observation Of Post-Synthesis Self-Narrowing Of The Particle Size Distribution. *Adv. Mat.,* 15, 1844-1849.

Hoffmann, E. & Pentel, P. 2000. PbS: From Solids To Clusters. *International Symposium On Structures And Dynamics Of Heterogeneous Systems*, 148-155.

Holke, A. & Henderson, H.T. 1999. Ultra-deep anisotropic etching of (110) silicon. *J. Micromech. Microeng.,* 9, 51-57.

Jackson, D. F. & Hawkes, D. J. 1981. X-Ray Attenuation Coefficient Of Elements And Mixtures. *Physics Reports,* 70, 169-233.

Lehmann, V., Stengl, R. & Luigart, A. 2000. On The Morphology And The Electrochemical Formation Mechanism Of Mesoporous Silicon. *Mat. Sci. Engr. B,* 69 - 70, 11 - 22.

Liu, J., Nelson, W. & Seefred, R. 2000. Response Calculations Of The CdZnTe Detector Using EGS4. SLAC.

Moreels, I., Lambert, K., Smeets, D., De Muynck, D., Nollet, T., Martins, J., Vanhaecke, F., Vantomme, A., Delerue, C., Allan, G. & Hens, Z. 2009. Size-Dependent Optical Properties Of Colloidal PbS Quantum Dots. *ACS Nano,* 3, 3023 - 3030.

Nassalski, A., Kapusta, M., Batsch, T., Wolski, D., Mockel, D., Enghardt, W. & Moszynski, M. 2007. Comparative Study Of Scintillators For PET/CT Detectors. *IEEE Transactions In Nuclear Science* 54, 3-10.

Nedelikovic, J. M., Patel, R. C., Kaufman, P., Joyce-Purden, C. & O'Leary, N. 1993. Synthesis And Optical Properties Of Quantum-Size Metal Sulfide Particles In Aqueous Solution. *J. Chem. Ed.,* 70, 342 - 344.

Owens, A. & Peacock, A. 2004. Compound Semiconductor Radiation Detectors. *Nuclear Instrumentation And Methods In Physics Research A*, 531, 18-37.

Perkins, J., Krawczynski, H. & Dowkontt, P. Characterizing Imarad CZT Detectors With Time Resolved Anode And Cathode. Proceedings Of The 13th International IEEE Workshop On Room-Temperature Semiconductor X- And Gamma-Ray Detectors 2003.

Sambur, J., Novet, T. & Parkinson, B. A. 2010. Multiple Exciton Collection In A Sensitized Photovoltaic System. *Science,* 330.

Schwenn, P. E., Watt, A. A. R., Rubinsztein-Dunlop, H. & Meredith, P. Lead Sulfide Nanocrystal/Conducting Polymer Solar Cell. SPIE, 2005.

Steigerwald, M. L. & Brus, L. E. 1990. Semiconductor Crystallites: A Class Of Large Molecules. *Acc. Chem. Res.,* 23, 183 - 188.

Taylor, M. L., Franich, R. D., Trapp, J. V. & Johnston, P. N. 2009. Electron Interaction With Gel Dosimeter: Effective Atomic Numbers For Collisional, Radiative, And Total Interaction Processes. *Radiation Research,* 171, 123-126.

Winder, C. & Sariciftci, N.S. 2004. Low bandgap polymers for photon harvesting in bulk heterojunction solar cells. *J. Mater. Chem.,* 14, 1077-1086.

Wong, K. H., Gruionu, L. G., Cheng, P., Abshire, P., Saveliev, V., Mun, S. K., Cleary, K. & Weinberg, I. N. PETglove: A New Technology For Portable Molecular Imaging. SPIE Medical Imaging Conference 2006.
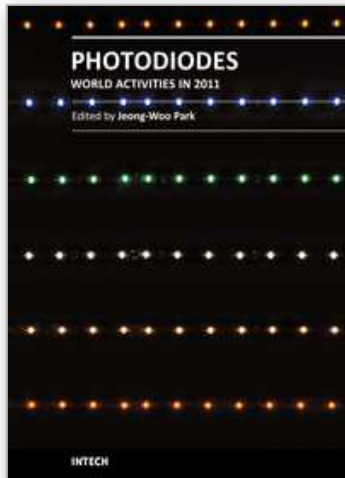
Photodiodes - World Activities in 2011

Edited by Prof. Jeong Woo Park

Photodiodes or photodetectors are in one boat with our human race. Efforts of people in related fields are contained in this book. This book would be valuable to those who want to obtain knowledge and inspiration in the related area.

How to reference

In order to correctly reference this scholarly work, feel free to copy and paste the following:

Mario Urdaneta, Pavel Stepanov, Irving Weinberg, Irina Pala and Stephanie Brock (2011). Quantum Dot Composite Radiation Detectors, Photodiodes - World Activities in 2011, Prof. Jeong Woo Park (Ed.), ISBN: 978-953-307-530-3, InTech, Available from: http://www.intechopen.com/books/photodiodes-world-activities-in-2011/quantum-dot-composite-radiation-detectors

INTECH
open science | open minds